Available online at www.sciencedirect.com

ScienceDirect

www.elsevier.com/locate/jes

JES JOURNAL OF ENVIRONMENTAL SCIENCES

www.jesc.ac.cn

Research Article

Acetylacetone effectively controlled the secondary metabolites of *Microcystis aeruginosa* under simulated sunlight irradiation

Xiaomeng Wang[1,**,*], *Yixin Luo*[1,**], *Shujuan Zhang*[2], *Lixiang Zhou*[1]

[1] *Department of Environmental Engineering, College of Resources and Environmental Sciences, Nanjing Agricultural University, Nanjing 210095, China*

[2] *The State Key Laboratory of Pollution Control and Resource Reuse, School of the Environment, Nanjing University, Nanjing 210023, China*

ARTICLE INFO

Article history:
Received 30 September 2022
Revised 2 December 2022
Accepted 3 December 2022
Available online 14 December 2022

Keywords:
Microcystis aeruginosa
Photodegradation
Acetylacetone
Secondary metabolites
Microcystin

ABSTRACT

Inactivation of cyanobacterial cells and simultaneous control of secondary metabolites is of significant necessity for the treatment of cyanobacteria-laden water. Acetylacetone (AcAc) has been reported a specific algicide to inactivate *Microcystis aeruginosa* (*M. aeruginosa*) and an effective light activator to degrade pollutants. This study systematically investigated the photodegradation ability of AcAc under xenon (Xe) irradiation on the secondary metabolites of *M. aeruginosa*, mainly algal organic matter (AOM), especially toxic microcystin-LR (MC-LR). Results showed that AcAc outperformed H_2O_2 in destructing the protein-like substances, humic acid-like matters, aromatic proteins and fulvic-like substances of AOM. For MC-LR (250 μg/L), 0.05 mmol/L AcAc attained the same degradation efficiency (87.0%) as 0.1 mmol/L H_2O_2. The degradation mechanism of Xe/AcAc might involve photo-induced energy/electron transfer and formation of carbon center radicals. Alkaline conditions (pH > 9.0) were detrimental to the photoactivity of AcAc, corresponding to the observed degradation rate constant (k_1 value) of MC-LR drastically decreasing to 0.0013 min^{-1} as solution pH exceeded 9.0. The PO_4^{3-} and HCO_3^- ions had obvious inhibition effects, whereas NO_3^- slightly improved k_1 value from 0.0277 min^{-1} to 0.0321 min^{-1}. The presence of AOM did not significantly inhibit MC-LR degradation in Xe/AcAc system. In addition, the biological toxicity of MC-LR was greatly reduced after photoreaction. These results demonstrated that AcAc was an alternative algicidal agent to effectively inactivate algal cells and simultaneously control the secondary metabolites after cell lysis. Nevertheless, the concentration and irradiation conditions should be further optimized in practical application.

Introduction

In recent years, cyanobacteria blooms caused by eutrophication of water bodies are frequently occurring in lakes

* Corresponding author.
E-mail: wangxiaomeng@njau.edu.cn (X. Wang).
** These authors contributed equally to this work.

https://doi.org/10.1016/j.jes.2022.12.004
1001-0742/

and reservoirs. They usually increase turbidity and produce taste and odor-causing compounds, presenting aesthetic and water quality challenges to drinking water authorities (Boyd et al., 2000; Fahnenstiel et al., 2008). Contaminated water by cyanobacteria, especially *Microcystis aeruginosa* (*M. aeruginosa*) which is one of the most common cyanobacteria, usually contains abundant algae cells, algal organic matters (AOM), and toxic metabolites (Zhang et al., 2019a). The proliferation of algal population and the death of algal cells deplete most of the dissolved oxygen, thereby limiting the growth of other organisms and leading to reduced biodiversity (Misra, 2011). The algae-laden water causes serious pollution to environment and brings many difficulties to water treatment.

For now, many methods have been proposed to control cyanobacterial blooming. Limiting nutrients such as nitrogen and phosphorus in water sources is an essential long-term strategy (Jancula and Marsalek, 2011). Short-term chemical remediation measures are often used to reduce cyanobacterial proliferation due to their effectiveness and economy (Matthijs et al., 2016). Using chemical algicide is the most effective way, and the common algicides include metals (e.g., copper sulfate, $CuSO_4$), oxidants (e.g., hydrogen peroxide, H_2O_2), herbicides (e.g., diuron), and natural compound-derived chemicals (e.g., ethyl 2-methylacetoacetate, EMA) (Matthijs et al., 2016; Xu et al., 2019; Zhang et al., 2016; Zhou et al., 2013). These algicidal chemicals effectively control cyanobacterial growth via the mechanisms of inhibiting photosynthesis-related a gene transcription, blocking the electron transport chain, or overwhelming the antioxidant system (Giacomazzi and Cochet, 2004; Qian et al., 2010). However, the intense cyanobacterial inactivation is usually accompanied by severe cell lysis, which inevitably leads to the release of large amounts of intracellular metabolites (Ma et al., 2012). For example, Zhou et al. (2013) reported that $CuSO_4$, H_2O_2, diuron, and EMA all induced severe cell lysis of *M. aeruginosa* and increased the concentration of extracellular microcystin-LR (MC-LR). Undoubtedly, the release of toxic metabolites to surrounding environment inevitably causes secondary pollution. Algae-related organic matters will significantly aggravate the burden of water purification, such as increasing coagulant dose, aggravating membrane fouling, and forming disinfection byproducts (Henderson et al., 2010). In particular, microcystins (MCs) pose a serious threat to human health because of high hepatotoxicity and tumorigenicity (Karner et al., 2001). Due to the cyclic structure, they are very chemically stable and can exist stably in aqueous environment for a long time (Zhang et al., 2010). Therefore, inactivation of algal cells with simultaneously controlling secondary metabolites is of significant necessity for the treatment of cyanobacteria-containing waters.

Acetylacetone (AcAc), a small molecule diketone naturally existing in fruits and vegetables, has been reported a specific algicide for the freshwater cyanobacteria (Yilimulati et al., 2021, 2022). As an algicide, AcAc has better biocompatibility with many other living systems in environment and is much cheaper than most allelochemicals (Yilimulati et al., 2021). Compared with H_2O_2, AcAc with a lower dose (0.1 mmol/L) is effective, and its inhibitory effect is longer lasting. H_2O_2 inactivates cyanobacterial cells by oxidative stress (Zhang et al., 2019b), whereas AcAc inhibits cyanobacterial growth through a nonoxidative pathway (Yilimulati et al., 2022). Specifically, AcAc acts on *M. aeruginosa* via selectively interfering with photosynthetic electron transport chain by targeting nonheme iron in Photosystem II (PSII) and the iron–sulfur clusters in ferredoxin (Yilimulati et al., 2021). Furthermore, AcAc has been reported to be a photo-activator that can mediate the redox of various pollutants (Dong et al., 2019; Zhang et al., 2014). Our previous study preliminary confirmed that AcAc could effectively degrade MCs under sunlight irradiation (Wang et al., 2018). In a coagulation system mediated by AcAc-embedded titanium xerogel coagulant (TXC), 0.07 mmol/L AcAc (released from TXC structure) reduced extracellular MCs from 40 μg/L (in control set) to 7 μg/L over a 16-day period (Wang et al., 2018). Benefiting from its photoactivity, AcAc may be a promising alternative algicide for the treatment of algae-containing waters with the advantages of inactivating algal cells and simultaneously controlling secondary metabolites. For this purpose, its photoactivity to the secondary metabolites deserves an in-depth study.

In recent years, the photoactivity of AcAc has attracted extensive attention and research. The high photoactivity of AcAc stems from its enol form, not the keto structure (Zhang et al., 2021). AcAc is highly efficient in decoloring dyes (Wang et al., 2013), degrading pharmaceuticals (Zhang et al., 2017), synchronously oxidizing As(III) and reducing nitrate (Chen et al., 2017), and decomplexing Cu-EDTA compound (Zhang et al., 2019c). The high photoactivity of AcAc differs from H_2O_2-based advanced oxidation process characterized by strong oxidizing reactive species (Pan et al., 2018). The possible degradation mechanisms involve three aspects: (1) direct energy/electron transfer occurring within the AcAc-substrate complexes (Wu et al., 2020a; Zhang et al., 2017), (2) formation of carbon center radicals, such as CH_3•, $CH_3C(O)$•, $CH_3C(O)CH_2$•, etc. (Wu et al., 2020a), and (3) as an electron shuttle for redox conversion (Chen et al., 2017). The photoactivity of AcAc is closely affected by solution pH, light intensity, and concentration (Luo et al., 2022; Wang et al., 2013). These preliminary results will help to reveal the degradation efficiency and related mechanism of AcAc on the secondary metabolites of *M. aeruginosa* under sunlight irradiation.

In this study, we systematically investigate the photodegradation performance of AcAc toward secondary metabolites under simulated sunlight irradiation. The main objectives are to (1) explore the degradation efficiencies of the secondary metabolites, especially the toxic MCs, (2) assess the effects of water quality parameters, (3) elucidate the degradation mechanism of AcAc, and (4) identify the toxicity change after photoreaction. The outcomes of this study will shed light on the potential application of AcAc in algal pollution control.

1. Materials and methods

1.1. Materials and reagents

MC-LR (≥ 95% by HPLC) was purchased from Taiwan Algal Science Inc. Trifluoroacetic acid (TFA) was obtained from Macklin Reagent Co., China. Acetonitrile and formic acid (FA) of chromatographic grade were purchased from Merck and used as received. Protein phosphatase enzyme (PP1), bovine

serum, dithiothreitol, *p*-nitrophenyl phosphate and Tri-HCl were purchased from Sigma-Aldrich Co., USA. Other chemicals, including AcAc, H_2O_2 (30%, *V/V*), $HClO_4$, NaOH, $NaNO_3$, Na_3PO_4, and $NaHCO_3$ were purchased from Sinopharm Chemical Reagent Co., Ltd., China. The actual water was obtained from Taihu Lake in April, and its water quality parameters were as follows: pH: 7.3, organic carbon content: 6.5 mg/L, and conductivity: 497 μS/cm.

M. aeruginosa (strain FACHB-905) was purchased from Institute of Hydrobiology, Chinese Academy Science (Wuhan, China). Cyanobacteria were cultivated in sterile BG11 medium, and harvested after 28 days by centrifugation at 6000 ×*g* for 15 min. The supernatant was filtered through a 0.45 μm membrane to remove residual cells, and the filtrate was referred as extracellular organic matter (EOM). Cyanobacterial cells collected by centrifugation were resuspended with the same volume of deionized water, and then frozen at -28°C for 24 hr. After that, the mixture was digested via ultrasonication (200 W, 5 sec/5 sec) for 10 min and solid-liquid separation via centrifugation at 10000 ×*g* for 20 min. The intracellular organic matter (IOM) was obtained after filtration through a 0.22 μm membrane. The concentration of EOM and IOM was featured by dissolved organic carbon (DOC), which was measured with a total organic carbon (TOC)-L_{CSH} analyzer (Shimadzu Co., Japan).

1.2. *Photodegradation experiments*

Irradiation experiments were conducted in a rotating disk photoreactor (Nanjing Xujiang, China) equipped with a 250 W xenon (Xe) lamp. The equipment diagram of photoreaction process was shown in Appendix A Fig. S1, and the emission spectrum of Xe lamp was given in Appendix A Fig. S2. A volume of 25 mL solution containing a certain amount of AcAc or H_2O_2 (0.01-0.5 mmol/L) and pollutant were held in quartz tubes around the lamp. The condensate water was cycled to maintain temperature at 25°C. Prior to photoirradiation, solution pH was adjusted to the predetermined values (2.0-11.0) by adding $HClO_4$ or NaOH, and no longer controlled during degradation process. At predetermined intervals, 3 mL suspension was withdrawn for further analyses. A blank control without AcAc and H_2O_2 addition was also conducted in parallel.

To analyze the degradation mechanism, tert-butanol (TBA) or sorbic acid (SA) were added to the reaction system as scavenger of HO• radical or triplet state of AcAc, respectively. In addition, the photodegradation was also investigated under continuous N_2- or air-aeration conditions. Some representative inorganic ions and organic matters were used to investigate the effects of water quality parameters. Specifically, inorganic anions, including NO_3^-, PO_4^{3-} and HCO_3^-, were tested in the range of 1-10 mg/L, 0.5-5.0 mg/L and 1-5 mmol/L, respectively. The effect of organic matters on MC-LR degradation was investigated in AOM concentration range of 1-10 mg/L. In addition, photodegradation experiments were also carried out in diluted BG11 solution (10 ×) and actual Taihu water.

1.3. *Analytic methods*

MC-LR was determined with high-performance liquid chromatography (HPLC), which was performed on a Waters Alliance 1525 (Waters, USA) with a 2489 PDA detector and an Agilent Eclipse Plus C18 reverse-phase column (10 cm × 4.6 mm, 3.5 μm). The mobile phase was a mixture of 0.05% (*V/V*) trifluoroacetic acid (TFA) in acetonitrile solution (40%) and 0.05% (*V/V*) TFA in aqueous solution (60%). The injection volume was 50 μL and the flow rate was 0.2 mL/min. The wavelength of UV absorbance detector was 238 nm. AOM was analyzed by three-dimension excitation emission matrix fluorescence spectra (3D-EEM spectra) on a fluorescence spectrophotometer (Fluoromax-4, HORIBA Co., Germany). The excitation wavelength ranged from 200 to 500 nm, and the emission was in the range of 250-550 nm with 5 nm increments. EEM fluorescence spectroscopy was quantified by fluorescence regional integration (FRI) method according to a previous report (Chen et al., 2003).

The toxicity of degradation intermediates was evaluated with protein phosphatase assays (PP1), which were conducted using a modification of previously reported colorimetric procedures (Carmichael and An, 1999; Rodriguez et al., 2008). PP1 enzyme solution was diluted to ~0.05 unit/μL in a buffer of 50 mmol/L Tris-HCl, 10.0 g/L albumin from bovine serum (BSA), 1.0 mmol/L $MnCl_2$, and 2.0 mmol/L dithiothreitol (pH 7.4). A 5 mmol/L *p*-nitrophenyl phosphate standard solution was prepared in buffer containing 50 mmol/L Tri-HCl, 20 mmol/L $MgCl_2$, 0.2 mmol/L $MnCl_2$, and 0.5 g/L BSA with pH 8.1. All buffer solutions were freshly prepared. MC-LR and test samples were diluted with Milli-Q water. The specific experimental protocol was as follows. Test solution of 10 μL were added to 10 μL PP1 solution in a 96-well polystyrene microtiter plate. After a few seconds of gentle shaking, the microtiter plate was kept at room temperature for 5 min followed by addition of 180 μL *p*-nitrophenyl phosphate solution (substrate). The plate was incubated at 30°C and the production of *p*-nitrophenol was measured at 405 nm on a μQuant Microplate Reader (Bio Tek, USA) at 4 min intervals for 60 min. A dose dependent kinetic activity for PP1 against substrate was established to assess the enzyme activity prior to sample test. The inhibition of enzyme activity against a negative control of Milli-Q water was measured at known MC-LR concentrations to establish the PP1 inhibition curve. All enzyme assays were performed in triplicate.

2. Results and discussion

2.1. *Photodegradation of secondary metabolites by AcAc under simulated sunlight irradiation*

2.1.1. *Degradation efficiency of algae-related organic matters*

Aqueous AOM, derived from algal metabolites, typically include proteins, peptides, amino sugars, polysaccharose, and humic-like substances (Li et al., 2012; Pivokonsky et al., 2014). AOMs are generally categorized into EOM and IOM, and their main components are significantly different. The typical 3D-EEM spectrum of IOM presented a major peak located at the Excitation/Emission (Ex/Em) range of 270-290 nm/310-331 nm (Peak A) (Fig. 1a), which was a protein-like peak associated with tryptophan, tyrosine-like organic matter (amino acid, polypeptide and protein) (Yamashita and Tanoue, 2003). IOM might comprise of soluble microbial byproduct-like substances and aromatic protein-like substances, includ-

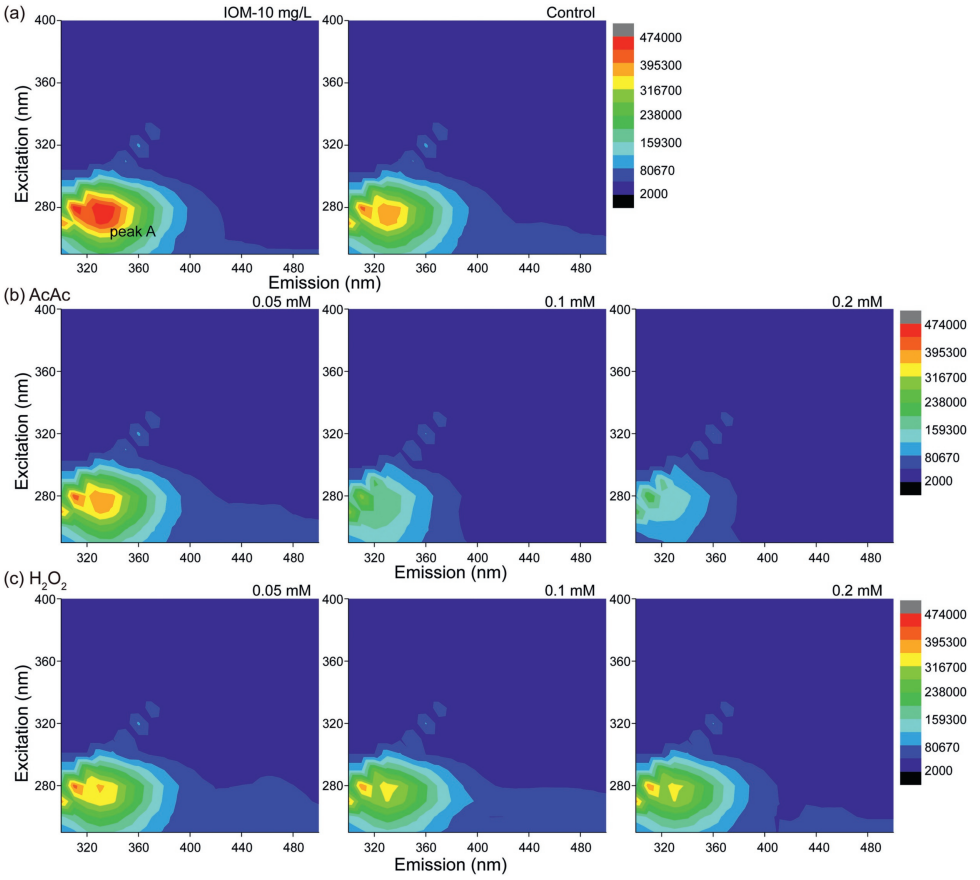

Fig. 1 – Variation of 3D-EEM spectra of IOM (10 mg-C/L) after irradiation for 60 min in three reaction systems: (a) sole Xe irradiation (control set), (b) Xe/AcAc systems, and (c) Xe/H_2O_2 systems. Initial solution pH: 7.5.

ing enzymes, MCs secreted from cyanobacteria, proteins or protein-like materials (Nelson et al., 1998). The EEM spectrum of EOM (Fig. 2a) exhibited a characteristic pattern distinct from IOM, presenting four main peaks. Besides the soluble microbial byproduct-like material (Region A), EOM had other humic-like substances (Region B), aromatic proteins (Region C), and fulvic-like substances (Region D). According to previous studies, the fluorescence substances in these regions might relate to bacterial decomposition products of cyanobacteria residue and secretion (Rochelle-Newall and Fisher, 2002).

Fig. 1a showed that Peak A of IOM was significantly declined after Xe lamp irradiation for 120 min. This might be attributed to the self-photosensitized reaction of dissolved organic matters (Ou et al., 2011; Page et al., 2011) and the phycocyanin photosensitized transformation (Song et al., 2007). In Xe/AcAc systems, the intensity of peak A was further decreased as AcAc concentration increased from 0.05 to 0.2 mmol/L (Fig. 1b). However, H_2O_2 with concentrations of 0.05-0.2 mmol/L did not significantly reduce the intensity of peak A compared with control set (Fig. 1c). We utilized fluorescence regional integration (FRI) to quantitatively analyze the kinetic variation in the intensity of Region A, and results were shown in Appendix A Fig. S3. Apparently, AcAc exhibited a great advantage over the equal-dosed H_2O_2 in degrading the protein-like constituents in algae-related organic matters.

Unlike IOM, EOM was not obviously degraded under sole xenon lamp irradiation (Fig. 2a). A significant degradation occurred in Xe/AcAc system (Fig. 2b), where the intensities of the four regions were drastically decreased, especially region B almost completely disappeared. H_2O_2 under xenon lamp irradiation only slightly decreased the intensity of protein-like substances (Region A) (Fig. 2c). These results indicated that EOM was more resistant to photodegradation than IOM. It was because some photoactive pigments in IOM, such as phycoyanin and chlorophyll a, might facilitate the degradation under light due to their photosensitization effects (Li et al., 2015). The addition of AcAc or H_2O_2 alone did not degrade IOM or EOM in the absence of Xe irradiation (data not shown). The different photodegradation abilities of AcAc and H_2O_2 toward AOM might arise from their different reaction mechanisms under light irradiation. It was well known that the strongly oxidized HO• radical was the main reactive specie involved in H_2O_2 photooxidation (Meng et al., 2022). The reaction velocities between HO• radical and natural organic matter were closely dependent on the molecular weight (MW), and the small organic molecules < 1 kDa had a high second-order reaction rate constant with HO• (Dong et al., 2010). Li et al. (2012) previously reported that MW fractions of IOM in < 1 kDa, 40-800 kDa, and > 800 kDa were 27%, 42%, and 31%, respectively, whereas EOM primarily contained 1-100 kDa molecules. These results implied that most of IOM and EOM was insensitive to HO• rad-

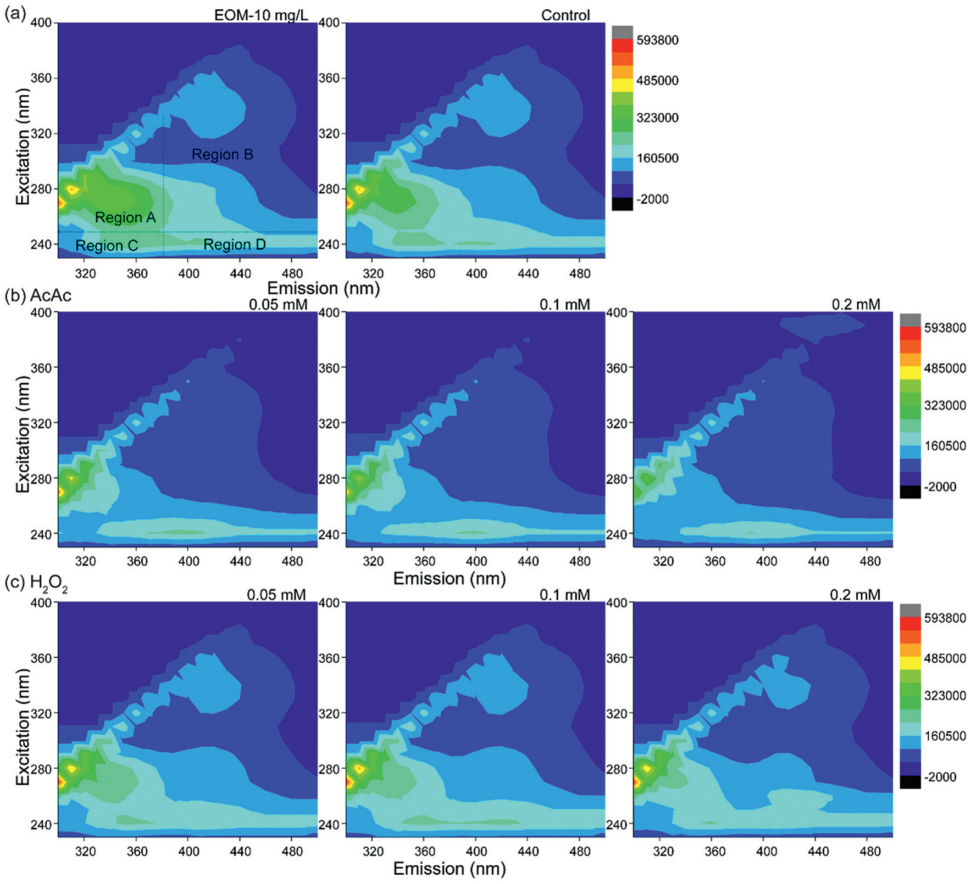

Fig. 2 – Variation of 3D-EEM spectra of EOM (10 mg-C/L) after irradiation for 60 min in three reaction systems: (a) sole Xe irradiation (control set), (b) Xe/AcAc systems, and (c) Xe/H_2O_2 systems. Initial solution pH: 7.5.

ical. In contrast, AcAc degraded organic pollutants through a different pathway (Liu et al., 2014). It might be the main reason for the high efficiency of AcAc in destroying algae-related organic matters.

2.1.2. *Removal of MC-LR*

Microcystins (MCs), the common toxins produced by cyanobacteria, receive more attention than algae-related organic matters due to the biotoxicity (Karner et al., 2001). MC-LR is the most common and most toxic structural variant of microcystins (Perez and Aga, 2005). The photodegradation ability of AcAc toward MC-LR under Xe lamp irradiation was investigated in concentration range of 0.01-0.5 mmol/L, and the results were given in Appendix A Fig. S4.

About 26.9% of MC-LR was removed after direct irradiation for 60 min. After addition of AcAc or H_2O_2, the degradation efficiency of MC-LR was remarkably improved. AcAc with concentration of 0.05 mmol/L removed approximate 87.0% of MC-LR, whereas the removal efficiency in H_2O_2 system at the equal dose was 70.0%. In addition, we found that the dose-dependent effects in AcAc and H_2O_2 systems were different. At AcAc dose below 0.05 mmol/L, a larger dose induced a higher degradation efficiency, but a further increase did not always bring about a continual promotion in removal efficiency (Appendix A Fig. S4a). This result was consistent with the photodegradation process of acid orange 7 by UV/AcAc, which might be attributed to the attenuation of the available light intensity (Gajdek et al., 2004; Zhang et al., 2014). In H_2O_2-photosystems, the degradation efficiency of MC-LR was continuously and significantly improved with the increase of H_2O_2 concentration (Appendix A Fig. S4b). The removal efficiency reached 98.8% at H_2O_2 concentration of 0.5 mmol/L after 60 min irradiation. In low concentration range (0.01-0.1 mmol/L), the pseudo-first-order degradation rate constants (k_1 values) in Xe/AcAc processes were larger than those in Xe/H_2O_2 systems (0.0201-0.0347 min^{-1} vs 0.011-0.0346 min^{-1}) (Fig. 3a). The same experimental phenomenon about the effect of AcAc/H_2O_2 concentration was also observed in our previous report (Zhang et al., 2014).

2.2. *Effects of water quality parameters on photodegradation of MC-LR*

2.2.1. *Solution pH*

The effect of solution pH was investigated in the range of 2.0-11.0. As shown in Fig. 3b, acidic conditions promoted MC-LR degradation by Xe/AcAc, whereas the oxidation ability of H_2O_2 was not significantly affected by solution pH. The alkaline condition (pH 9.0) slightly improved the degradation efficiency in Xe/H_2O_2 process (k_1 was 0.033 min^{-1}) (Fig. 3b),

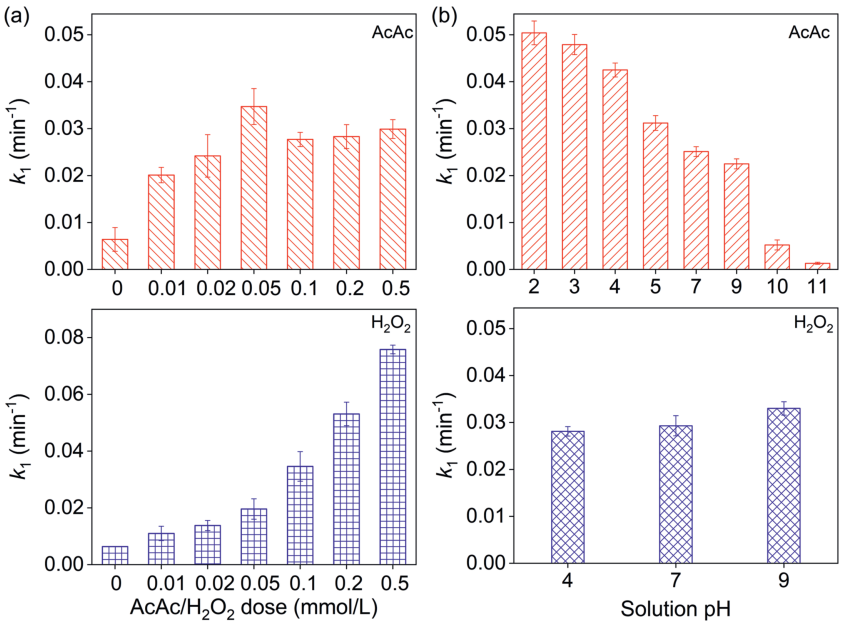

Fig. 3 – Degradation rate constants (k_1 values) of MC-LR (250 μg/L) in Xe/AcAc and Xe/H_2O_2 systems under different conditions. (a) Various doses of AcAc and H_2O_2. Initial solution pH: 7.5. (b) Different initial solution pH. AcAc: 0.1 mmol/L, H_2O_2: 0.1 mmol/L.

which might be attributed to the higher molar absorption coefficient of the peroxide anions under alkaline conditions (Legrini et al., 1993). However, the k_1 values in Xe/AcAc system reached maximal values (0.0425-0.0504 min^{-1}) at pH below 4.0, and decreased greatly when solution pH was above 9.0 (Fig. 3b). Previous studies indicated that AcAc had two tautomers, enol and keto forms (Nakanishi et al., 2006), and the protonated enol structure mainly contributed to light activation (Zhang et al., 2021). The acid dissociation equilibrium constant (pK_a) of AcAc was 9.0 (Stary and Liljenzin, 1982). Therefore, at pH ≥ 9.0, AcAc undergoes base-catalyzed ionization, leading to the formation of enolate ion (Mofaddel et al., 2004). Conversely, acidic conditions (pH < 4.0) facilitated the formation of protonated enol structure, consequently leading to a higher photoactivity. Previous studies also demonstrated that the decolorizing efficiencies of crystal violet by UV/AcAc under acidic conditions were much better than those under alkaline environment (Yang et al., 2021). These results indicated that the alkaline conditions would greatly limit the degradation of MC-LR by AcAc.

2.2.2. *Inorganic anions*

Eutrophication is usually caused by excessive contents of N and P nutrients. We investigated the effects of NO_3^-, PO_4^{3-}, and alkalinity (HCO_3^-), and the results were shown in Table 1. The k_1 values indicated that NO_3^- significantly promoted the degradation efficiency of MC-LR, whereas PO_4^{3-} and HCO_3^- greatly inhibited the photodegradation. The presence of NO_3^- also improved the degradation efficiency in solo xenon irradiation (control), with k_1 value increasing from 0.0064 min^{-1} (control set) to 0.0347 min^{-1} (10 mg/L NO_3^-). The degradation efficiency in Xe/H_2O_2 system was also improved as NO_3^- concentration increased to 10 mg/L (Appendix A Fig. S5), and

Table 1 – Effect of the inorganic NO_3^-, PO_4^{3-}, and HCO_3^- ions on the degradation rate constants (k_1 values) of MC-LR in Xe/AcAc and Xe/H_2O_2 systems. MC-LR: 250 μg/L, AcAc: 0.1 mmol/L, H_2O_2: 0.1 mmol/L, initial solution pH: 7.5.

Factors		k_1 value (min^{-1})		
		Xe	Xe/AcAc	Xe/H_2O_2
Control	0	0.0064	0.0277	0.0346
	1	0.0127	0.0278	0.0299
NO_3^--N (mg/L)	5	0.0319	0.0321	0.0417
	10	0.0347	0.0321	0.0491
	0.5	0.0059	0.011	0.039
PO_4^{3-}-P (mg/L)	2	0.0520	0.0069	0.0264
	5	0.0055	0.0055	0.0150
	1	0.0056	0.0048	0.0172
HCO_3^- (mmol/L)	2	0.0052	0.0050	0.0134
	5	0.0054	0.0055	0.0095

the effect of NO_3^- on Xe/H_2O_2 process was more significant than that in Xe/AcAc system (Table 1). The positive effects in Xe/H_2O_2 and Xe irradiation systems were attributed to the HO• and NO_2• radicals formed from the photolysis of NO_3^- under light irradiation (Goldstein et al., 2007; Li et al., 2022). However, in Xe/AcAc system, an inner filter effect simultaneously existed since NO_3^- not only strongly absorbs photons of wavelength shorter than 250 nm but also had a characteristic absorption peak close to AcAc (Wu et al., 2016a). In addition to the inner filter effect, the presence of NO_3^- was also detrimental to the energy/electron transfer between AcAc and pollutants (Wu et al., 2016a). Therefore, the presence of NO_3^- induced a less promotion to Xe/AcAc reaction than that in Xe/H_2O_2 system.

Both HCO_3^- and PO_4^{3-} inhibited the degradation efficiencies in Xe/AcAc and Xe/H_2O_2 systems (Appendix A Fig. S5), but their respective effects were different (Table 1). Obviously, the inhibitory effects of HCO_3^- and PO_4^{3-} on Xe/AcAc system were independent of their concentrations, in which a further increase of HCO_3^- and PO_4^{3-} concentration did not continuously deteriorate the degradation efficiency (Appendix A Fig. S5a). In AcAc photo reaction, the main degradation products of AcAc (several small molecular organic acids) usually caused a decline in solution pH (Wu et al., 2016b). However, the presence of HCO_3^- and PO_4^{3-} ions would inhibit the drop of solution pH. In Xe/AcAc system, the effluent pH was 5.4 after reaction for 60 min, whereas the presence of 1 mmol/L HCO_3^- or 0.5 mg/L PO_3^- maintained solution pH at 8.3 or 7.5. The inhibitory effects of HCO_3^- and PO_3^- on AcAc photodegradation might result from their influences on solution pH. On the contrary, the degradation efficiency in Xe/H_2O_2 system was continuously decreased as the concentrations of HCO_3^- and PO_4^{3-} increased (Appendix A Fig. S5b). Specifically, 5 mg/L PO_4^{3-} reduced k_1 value from 0.0346 min^{-1} to 0.0150 min^{-1}, while 5 mmol/L HCO_3^- reduced k_1 value to 0.0095 min^{-1} (Table 1). Their inhibitory effects originated from the competitive reaction with HO• radical (Xu et al., 2011). He et al., 2012 also found that the degradation kinetics of MC-LR in UV/H_2O_2 system in the presence of HCO_3^-/PO_4^{3-} significantly decreased owing to their scavenging effects on HO• specie. The reaction rate constant of HCO_3^- with HO• (8.5×10^6 $(mol/L)^{-1}$ sec^{-1}) is higher than that of PO_4^{3-} (1.5×10^5 $(mol/L)^{-1}$ sec^{-1}) (Ma et al., 2018), implying that the inhibitory effect of HCO_3^- was more pronounced than PO_4^{3-}.

2.2.3. *Algal organic matters*

Previous studies reported that AOM could degrade MC-LR under UV irradiation through a photosensitization mechanism, in which the phycocyanin was the main photosensitizer (Li et al., 2015). However, the presence of AOM might inhibit the photo-transformation efficiency of MC-LR via competing for reactive oxygen species (ROS) or adsorbing the photons (Jia et al., 2018; Li et al., 2015). As shown in Fig. 4a, the effects of AOM on these two photoreaction processes were significantly different. The equal dose of AOM performed much less influence on Xe/AcAc process. In Xe/AcAc system, k_1 value in the presence of 5 mg C/L AOM (0.0218 min^{-1}) was almost identical to that of AOM-free system (0.0243 min^{-1}), and it slightly decreased to 0.0158 min^{-1} as AOM increased to 10 mg C/L. However, the removal efficiency in Xe/H_2O_2 system was almost completely inhibited when AOM concentration was greater than 5 mg C/L, corresponding to the k_1 values of 0.0076 min^{-1} and 0.0063 min^{-1} at 5 and 10 mg C/L AOM, respectively. This result verified that the dissolved organic matter was a scavenger in advanced oxidation processes, which consumed partial HO• generated by H_2O_2 activation (Westerhoff et al., 2007).

2.2.4. *Actual water body*

In actual cyanobacterial bloom waters, the concentration of N was usually lower than 5.4 mg/L, and P concentration was in the range of 0.1-0.3 mg/L (Zhao et al., 2019). From the results in Table 1, they performed negligible effects on the photodegradation of MC-LR. However, algae-related organic matters in actual cyanobacterial bloom waters would cause a significant effect. Fig. 4b illustrated the degradation rates by Xe/AcAc and Xe/H_2O_2 in two actual waters (diluted culture solution and Taihu lake water). Results showed that the k_1 values in Xe/H_2O_2 system greatly decreased by 68.5-72.0% (from 0.0372 min^{-1} to 0.0104-0.0117 min^{-1}), whereas the photoactivity of AcAc did not decline drastically. As discussed above, solution pH was the key factor affecting the degradation efficiency in Xe/AcAc process. The inorganic anions might affect the pho-

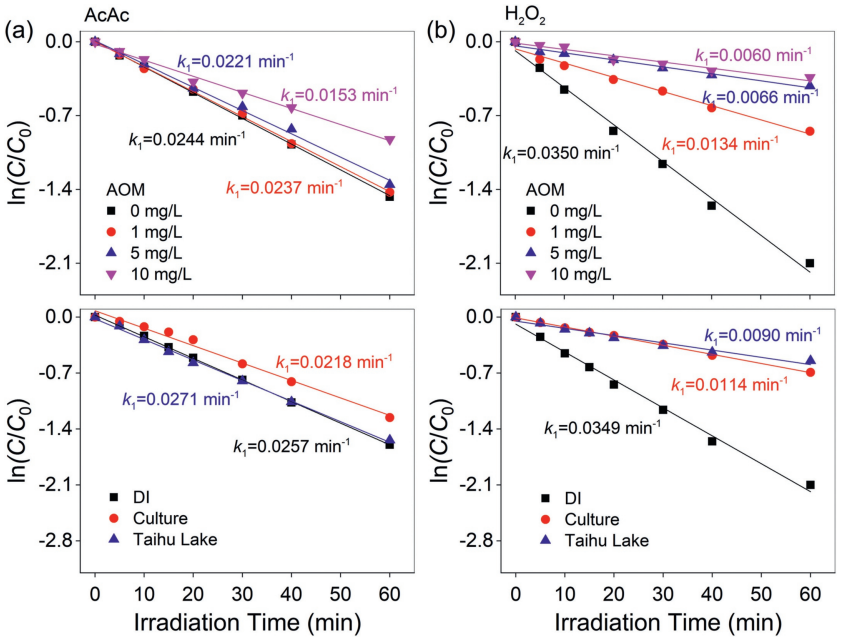

Fig. 4 – (a) Effect of AOM on the photodegradation of MC-LR in Xe/AcAc and Xe/H_2O_2 systems. (b) The degradation kinetics in diluted culture solution (10 x) and actual Taihu lake water. MC-LR: 250 μg/L, AcAc: 0.1 mmol/L, H_2O_2: 0.1 mmol/L, initial solution pH: 7.5.

todegradation of Xe/AcAc process through improving solution pH. Moreover, algae-related matters would not greatly inhibit the degradation efficiency of MC-LR. Compared with Xe/AcAc process, organic matter and some inorganic anions had significant inhibitory effects on MC-LR degradation in Xe/H_2O_2 system through competitive reaction with HO• radical. Therefore, in practical application, AcAc exhibited another significant advantage over H_2O_2 because of its strong resistance to complex water quality environment.

2.3. *Mechanism involved in the photodegradation of AcAc*

As we all know, HO• is the main reactive species involved in H_2O_2 photodegradation process. Fig. 5a verified that the addition of 10 mmol/L tert-butanol (TBA) as HO• scavengers completely inhibited the degradation efficiency of MC-LR in Xe/H_2O_2 system, whereas the TBA-quenching reaction had a minor effect on Xe/AcAc process (Fig. 5a). However, sorbic acid (SA), as the triplet excited state scavenger, completely inhibited the photodegradation by AcAc (Fig. 5b), indicating that the triplet state of AcAc (^{3}AcAc*) played a dominant role during AcAc photolysis. Zhang et al. (2017) proposed that direct energy transfer or exciplexes formation were the possible reactions between ^{3}AcAc* and tetracycline. In addition, carbon central radical may also be a degradation pathway. Many studies have found that small molecules of diketones such as butandione (BD, the simplest α-diketone) and acetylacetone (AcAc, the simplest β-diketone) can be photodissociated under light irradiation to produce various types of carbon center radicals (Antonov et al., 2019; Faust et al., 1997). Wu et al. (2020b) also detected the free radical signal in AcAc solution under UV light and found the presence of $CH_3C(O)$•. Likewise, the possible mechanism in Xe/AcAc process might involve direct energy/electron transfer between ^{3}AcAc* and MC-LR molecular or carbon centered radical reactions.

In addition, Fig. 5c further showed that the degradation rate of MC-LR under N_2 bubbling drastically improved from 0.0245 min^{-1} to 0.1177 min^{-1}, but air saturation (~20% oxygen) slightly reduced the k_1 value (0.0189 min^{-1}). This result indicated that oxygen inhibited the degradation efficiency in Xe/AcAc process. Previous studies reported that O_2 could quench excited triplets of AcAc and thus reduce its photoactivity (Abdel-Shafi and Wilkinson, 2000; Zhang et al., 2017). In addition, the organic radicals generated by excited triplet of AcAc could react with O_2 to form peroxide radicals, which possessed stronger oxidizing ability (Wu et al., 2020b; Zhang et al., 2021). From these results, we deduced that the degradation mechanisms in Xe/AcAc reaction might involve two aspects: (1) direct electron/energy transfer between triplet state of AcAc and MC-LR molecular, and (2) oxidation effect by the organic radicals, including carbon center radicals and peroxide radicals. The former might play a dominant role for the photodegradation of MC-LR by AcAc.

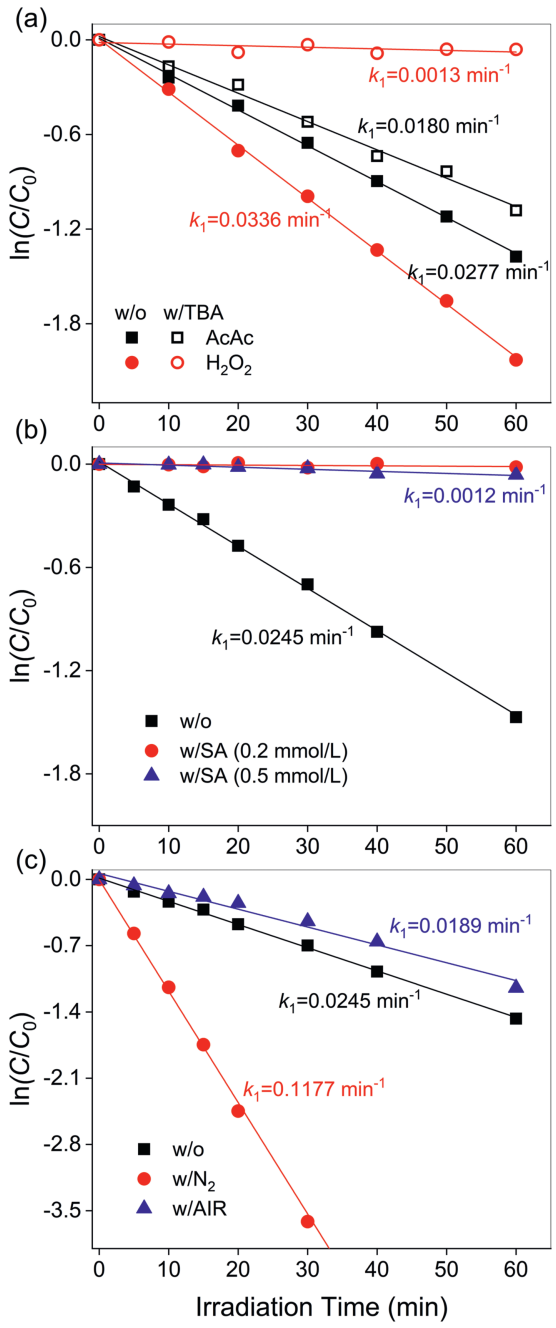

Fig. 5 – The degradation kinetics of MC-LR under different conditions. (a) In presence of 10 mmol/L tert-butanol (TBA) as hydroxyl radical scavenger. (b) The addition of sorbic acid (SA) as the triplet excited state scavenger. (c) Continuously aerated with N_2 or air. MC-LR: 250 μg/L, AcAc: 0.1 mmol/L, H_2O_2: 0.1 mmol/L, initial solution pH: 7.5.

2.4. *Toxicity assessment after photodegradation*

The chemical structure of MC-LR contains a unique amino acid, 3-amion-9-methoxy-2,6,8-trimethyl-10-phenyl-4,6-decadienoic acid (Adda). Adda is essential for the biotoxicity of MCs, and its geometrical isomers do not exhibit biological activity (Harada et al., 2004). MC-LR is a powerful inhibitor of important regulatory enzymes (protein phosphatase 1 and 2A) (Lee et al., 2004), and its ability to inhibit protein phosphatase 1 (PP1) directly reflect the biological toxicity. The kinetic variation of inhibitory rate (P/P_0) as well as the concentration degradation (C/C_0) were shown in Fig. 6. In sole irradiation system, P/P_0 performed a lower downtrend

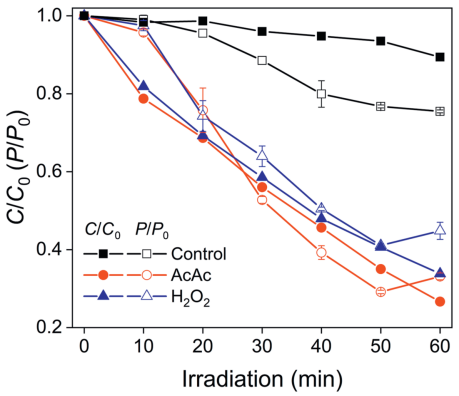

Fig. 6 – The variation rates of concentration (C/C_0) and inhibition on PP1 enzyme (P/P_0) in sole Xe irradiation (control set), Xe/AcAc, and Xe/H_2O_2 systems. MC-LR: 250 μg/L, AcAc or H_2O_2: 0.1 mmol/L, solution pH: 7.5.

than C/C_0. The decrease of toxicity might be because the direct photolysis of MC-LR resulted in the isomerization of intramolecular reaction (Li et al., 2016). Significantly, the inhibition rate in Xe/AcAc process was higher than the degradation efficiency of MC-LR. Isomerization of intramolecular reaction and destruction of the Adda moiety dramatically reduced the toxicity associated with MCs (Liu et al., 2003). On the contrary, only oxidation of diene bonds was involved in H_2O_2 oxidation process (Park et al., 2017). The result about toxicity assessment further demonstrated that AcAc exhibited a slightly advantage over H_2O_2 in reducing the biological toxicity of MC-LR.

In addition, the effect of the oxidizing agents on water safety is also of concern. H_2O_2 at effective doses had a certain impact on other invertebrates, bacteria and fishes (Wolf et al., 2018). AcAc was reported to have a low toxicity, corresponding to a high median lethal dose and lethal concentration (Liu et al., 2014). Furthermore, AcAc and its degradation products are small molecule organics, which can be used as carbon sources by microorganisms after photoreaction (Liu et al., 2014; Yang et al., 2018). Therefore, AcAc is an ecologically safe chemical used to control algal bloom and secondary metabolites.

3. Conclusions

AcAc could effectively control the secondary metabolites of *M. aeruginosa* under simulated sunlight irradiation, including algae-related organic matters and microcystins. In comparison to H_2O_2 photooxidation, AcAc significantly reduced the contents of protein-like substances, humic acid-like matters, aromatic proteins and fulvic-like substances in AOM, whereas the equal dose of H_2O_2 was quite inefficient. As for MC-LR, a lower dose of AcAc (0.05 mmol/L) reached the same degradation efficiency with 0.1 mmol/L H_2O_2. The photodegradation of AcAc was closely related to solution pH, and acidic conditions ($pH \leq 4.0$) were more favorable than alkaline solution ($pH > 9.0$). The presence of AOM performed a negligible effect on the removal efficiency of MC-LR by Xe/AcAc, while PO_4^{3-} and HCO_3^- ions inhibited the degradation process by elevating solution pH. The main degradation mechanism of Xe/AcAc process involved photo-induced energy/electron transfer. Isomerization of intramolecular reaction and destruction of the Adda moiety contributed to the reduction in biological toxicity of MC-LR during Xe/AcAc photodegradation. With environment-friendly property, AcAc was an available algicidal agent to dispose the cyanobacteria-laden water, which could effectively inactivate algal cells and simultaneously control the secondary metabolites after cell lysis. In practical application, the concentration and irradiation conditions should be further optimized.

Declaration of Competing Interest

The authors declare that they have no known competing financial interests or personal relationships that could have appeared to influence the work reported in this paper.

Acknowledgments

This work was supported by the National Natural Science Foundation of China (No. 21906085), the Natural Science Foundation of Jiangsu Province of China (No. BK20190547), and the State Key Laboratory of Pollution Control and Resource Reuse Foundation (No. PCRRF21046).

Appendix A Supplementary data

Supplementary material associated with this article can be found, in the online version, at doi:10.1016/j.jes.2022.12.004.

REFERENCES

Abdel-Shafi, A.A., Wilkinson, F., 2000. Charge transfer effects on the efficiency of singlet oxygen production following oxygen quenching of excited singlet and triplet states of aromatic hydrocarbons in acetonitrile. J. Phys. Chem. A 104, 5747–5757.

Antonov, I., Voronova, K., Chen, M.W., Sztaray, B., Hemberger, P., Bodi, A., et al., 2019. To boldly look where no one has looked before: identifying the primary photoproducts of acetylacetone. J. Phys. Chem. A 123, 5472–5490.

Boyd, P.W., Watson, A.J., Law, C.S., Abraham, E.R., Zeldis, J., 2000. A mesoscale phytoplankton bloom in the polar Southern Ocean stimulated by iron fertilization. Nature 407, 695–702.

Carmichael, W.W., An, J.S., 1999. Using an enzyme linked immunosorbent assay (ELISA) and a protein phosphatase inhibition assay (PPIA) for the detection of microcystins and nodularins. Nat. Toxins 7, 377–385.

Chen, W., Westerhoff, P., Leenheer, J.A., Booksh, K., 2003. Fluorescence excitation-Emission matrix regional integration to quantify spectra for dissolved organic matter. Environ. Sci. Technol. 37, 5701–5710.

Chen, Z.H., Song, X.J., Zhang, S.J., Wu, B.D., Zhang, G.Y., Pan, B.C., 2017. Acetylacetone as an efficient electron shuttle for concerted redox conversion of arsenite and nitrate in the opposite direction. Water Res. 124, 331–340.

Dong, M.M., Mezyk, S.P., Rosario-Ortiz, F.L., 2010. Reactivity of effluent organic matter (EfOM) with hydroxyl radical as a function of molecular weight. Environ. Sci. Technol. 44, 5714–5720.
Dong, Y.N., Wei, S.J., Wu, B.D., Zhang, S.J., 2019. Substituent effects on the photochemistry of acetylacetone in aqueous solutions. Environ. Chem. 38, 254–262.
Fahnenstiel, G.L., Millie, D.F., Dyble, J., Litaker, R.W., Tester, P.A., McCormick, M.J., et al., 2008. Microcystin concentrations and cell quotas in Saginaw Bay. Lake Huron. Aquat. Ecosyst. Health Manage. 11, 190–195.
Faust, B.C., Powell, K., Rao, C.J., Anastasio, C., 1997. Aqueous-phase photolysis of biacetyl (an alpha-dicarbonyl compound): A sink for biacetyl, and a source of acetic acid, peroxyacetic acid, hydrogen peroxide, and the highly oxidizing acetylperoxyl radical in aqueous aerosols, fogs, and clouds. Atmos. Environ. 31, 497–510.
Gajdek, P., Bober, B., Mej, E., Bialczyk, J., 2004. Sensitised decomposition of microcystin-LR using UV radiation. J. Photochem. Photobiol., B 76, 103–106.
Giacomazzi, S., Cochet, N., 2004. Environmental impact of diuron transformation: A review. Chemosphere 56, 1021–1032.
Goldstein, S., Aschengrau, D., Diamant, Y., Rabani, J., 2007. Photolysis of aqueous H_2O_2: Quantum yield and applications for polychromatic UV actinometry in photoreactors. Environ. Sci. Technol. 41, 7486–7490.
Harada, K., Imanishi, S., Kato, H., Mizuno, M., Ito, E., Tsuji, K., 2004. Isolation of Adda from microcystin-LR by microbial degradation. Toxicon 44, 107–109.
He, X.X., Pelaez, M., Westrick, J.A., O'Shea, K.E., Hisfeia, A., Triantis, T., et al., 2012. Efficient removal of microcystin-LR by UV-C/H_2O_2 in synthetic and natural water samples. Water Res. 46, 1501–1510.
Henderson, R.K., Parsons, S.A., Jefferson, B., 2010. The impact of differing cell and algogenic organic matter (AOM) characteristics on the coagulation and flotation of algae. Water Res. 44, 3617–3624.
Jancula, D., Marsalek, B., 2011. Critical review of actually available chemical compounds for prevention and management of cyanobacterial blooms. Chemosphere 85, 1415–1422.
Jia, P.L., Zhou, Y.P., Zhang, X.F., Zhang, Y., Dai, R.H., 2018. Cyanobacterium removal and control of algal organic matter (AOM) release by UV/H_2O_2 pre-oxidation enhanced Fe(II) coagulation. Water Res. 131, 122–130.
Karner, D.A., Standridge, A.J.H., Harrington, G.W., Barnum, R.P., 2001. Microcystin algal toxins in source and finished drinking water. J. AM. Water Works Ass. 93, 72–81.
Lee, D.K., Kim, S.C., Kim, S.J., Chung, I.S., Kim, S.W., 2004. Photocatalytic oxidation of microcystin-LR with TiO_2-coated activated carbon. Chem. Eng. J. 102, 93–98.
Legrini, O., Oliveros, E., Braun, A.M., 1993. Photochemical processes for water treatment. Chem. Rev. 93, 671–698.
Li, L., Gao, N.Y., Deng, Y., Yao, J.J., Zhang, K.J., 2012. Characterization of intracellular & extracellular algae organic matters (AOM) of *Microcystic aeruginosa* and formation of AOM-associated disinfection byproducts and odor & taste compounds. Water Res. 46, 1233–1240.
Li, L., Guo, H.C., Shao, C., Yu, S.L., Yin, D.Q., Gao, N.Y., et al, ., 2015. Effect of algal organic matter (AOM) extracted from *Microcystis aeruginosa* on photo-degradation of diuron. Chem. Eng. J. 281, 265–271.
Li, W.Y., Liu, Y., Sun, X.L., Wang, F., Qian, L., Xu, C., et al., 2016. Photocatalytic degradation of MC-LR in water by the UV/TiO_2/H_2O_2 process. Water Sci. Technol.: Water Supply 16, 34–43.
Li, Z.Q., Luo, C.W., Tan, F.X., Wu, D.J., Zhai, X.D., Wang, S.S., et al., 2022. UV light irradiation combined with nitrate for degradation of bisphenol A: kinetics, transformation pathways, and acute toxicity assessment. Environ. Sci.: Water Res. Technol. 8, 586–596.
Liu, I., Lawton, L.A., Robertson, P.K.J., 2003. Mechanistic studies of the photocatalytic oxidation of microcystin-LR: An investigation of byproducts of the decomposition process. Environ. Sci. Technol. 37, 3214–3219.
Liu, X.T., Song, X.J., Zhang, S.J., Wang, M.S., Pan, B.C., 2014. Non-hydroxyl radical mediated photochemical processes for dye degradation. Phys. Chem. Chem. Phys. 16, 7571–7577.
Luo, Y.X., Yang, J.W., Wang, X.M., Zhou, L.X., 2022. Acetylacetone promoted high-efficiency coagulation toward arsenite through a synchronous photooxidation process. Environ. Sci.: Water Res. Technol. 8, 1048–1058.
Ma, J., Yang, Y.Q., Jiang, X.C.H., Xie, Z.T., Li, X.X., Chen, C.Z., et al., 2018. Impacts of inorganic anions and natural organic matter on thermally activated persulfate oxidation of BTEX in water. Chemosphere 190, 296–306.
Ma, M., Liu, R.P., Liu, H.J., Qu, J.H., 2012. Chlorination of *Microcystis aeruginosa* suspension: Cell lysis, toxin release and degradation. J. Hazard. Mater. 217, 279–285.
Matthijs, H.C.P., Jancula, D., Visser, P.M., Marsalek, B., 2016. Existing and emerging cyanocidal compounds: New perspectives for cyanobacterial bloom mitigation. Aquat. Ecol. 50, 443–460.
Meng, X.Q., Li, F.J., Yi, L., Dieketseng, M.Y., Wang, X.M., Zhou, L.X., et al., 2022. Free radicals removing extracellular polymeric substances to enhance the degradation of intracellular antibiotic resistance genes in multi-resistant Pseudomonas Putida by UV/H_2O_2 and UV/peroxydisulfate disinfection processe. J. Hazard. Mater. 430, 128502.
Misra, A.K., 2011. Modeling the depletion of dissolved oxygen due to algal bloom in a lake by taking Holling type-III interaction. Appl. Math. Comput. 217, 8367–8376.
Mofaddel, N., Bar, N., Villemin, D., Desbene, P.L., 2004. Determination of acidity constants of enolisable compounds by capillary electrophoresis. Anal. Bioanal. Chem. 380, 664–668.
Nakanishi, H., Morita, H., Nagakura, S., 2006. Electronic structures and spectra of the keto and enol forms of acetylacetone. B. Chem. Soc. JPN. 50, 2255–2261.
Nelson, N.B., Siegel, D.A., Michaels, A.F., 1998. Seasonal dynamics of colored dissolved material in the Sargasso Sea. Deep Sea Res., Part I 45, 931–957.
Ou, H.S., Gao, N.Y., Deng, Y., Wang, H., Zhang, H.X., 2011. Inactivation and degradation of *Microcystis aeruginosa* by UV-C irradiation. Chemosphere 85, 1192–1198.
Page, S.E., Arnold, W.A., McNeill, K., 2011. Assessing the contribution of free hydroxyl radical in organic matter-sensitized photohydroxylation reactions. Environ. Sci. Technol. 45, 2818–2825.
Pan, M.W., Wu, Z.H., Tang, C.Y., Guo, K.H., Cao, Y.J., Fang, J.Y., 2018. Emerging investigators series: Comparative study of naproxen degradation by the UV/chlorine and the UV/H_2O_2 advanced oxidation processes. Environ. Sci.: Water Res. Technol. 4, 1219–1230.
Park, J.A., Yang, B., Park, C., Choi, J.W., van Genuchten, C.M., Lee, S.H., 2017. Oxidation of microcystin-LR by the Fenton process: Kinetics, degradation intermediates, water quality and toxicity assessment. Chem. Eng. J. 309, 339–348.
Perez, S., Aga, D.S., 2005. Recent advances in the sample preparation, liquid chromatography tandem mass spectrometric analysis and environmental fate of microcystins in water. TrAC, Trends Anal. Chem. 24, 658–670.
Pivokonsky, M., Safarikova, J., Baresova, M., Pivokonska, L., Kopecka, I., 2014. A comparison of the character of algal extracellular versus cellular organic matter produced by cyanobacterium, diatom and green alga. Water Res. 51, 37–46.

Qian, H.F., Yu, S.Q., Sun, Z.Q., Xie, X.C., Liu, W.P., Fu, Z.W., 2010. Effects of copper sulfate, hydrogen peroxide and N-phenyl-2-naphthylamine on oxidative stress and the expression of genes involved photosynthesis and microcystin disposition in *Microcystis aeruginosa*. Aquat. Toxicol. 99, 405–412.

Rochelle-Newall, E.J., Fisher, T.R., 2002. Production of chromophoric dissolved organic matter fluorescence in marine and estuarine environments: An investigation into the role of phytoplankton. Mar. Chem. 77, 7–21.

Rodriguez, E.M., Acero, J.L., Spoof, L., Meriluoto, J., 2008. Oxidation of MC-LR and -RR with chlorine and potassium permanganate: Toxicity of the reaction products. Water Res. 42, 1744–1752.

Song, W.H., Bardowell, S., O'Shea, K.E., 2007. Mechanistic study and the influence of oxygen on the photosensitized transformations of microcystins (cyanotoxins). Environ. Sci. Technol. 41, 5336–5341.

Stary, J., Liljenzin, J.O., 1982. Critical evaluation of equilibrium constants involving acetylacetone and its metal chelates. Pure Appl. Chem. 54, 2557–2592.

Wang, M.S., Liu, X.T., Pan, B.C., Zhang, S.J., 2013. Photodegradation of Acid Orange 7 in a UV/acetylacetone process. Chemosphere 93, 2877–2882.

Wang, X.M., Wang, X., Wei, Z.B., Zhang, S.J., 2018. Potent removal of cyanobacteria with controlled release of toxic secondary metabolites by a titanium xerogel coagulant. Water Res. 128, 341–349.

Westerhoff, P., Mezyk, S.P., Cooper, W.J., Minakata, D., 2007. Electron pulse radiolysis determination of hydroxyl radical rate constants with Suwannee river fulvic acid and other dissolved organic matter isolates. Environ. Sci. Technol. 41, 4640–4646.

Wolf, R., Thrane, J.E., Hessen, D.O., Andersen, T., 2018. Modelling ROS formation in boreal lakes from interactions between dissolved organic matter and absorbed solar photon flux. Water Res. 132, 331–339.

Wu, B.D., Yin, R., Zhang, G.Y., Yu, C., Zhang, S.J., 2016a. Effects of water chemistry on decolorization in three photochemical processes: Pro and cons of the UV/AA process. Water Res. 105, 568–574.

Wu, B.D., Yu, S.Y., Zhang, G.Y., Zhang, S.J., Shen, P.F., Tratnyek, P.G., 2020a. Role of complexation in the photochemical reduction of chromate by acetylacetone. J. Hazard. Mater. 400, 123306.

Wu, B.D., Zhang, G.Y., Zhang, S.J., 2016b. Fate and implication of acetylacetone in photochemical processes for water treatment. Water Res. 101, 233–240.

Wu, B.D., Zhang, L., Wei, S.J., Ou'Yang, L.X., Yin, R., Zhang, S.J., 2020b. Reduction of chromate with UV/diacetyl for the final effluent to be below the discharge limit. J. Hazard. Mater. 389, 121841.

Xu, H., Xu, W.G., Wang, J.F., 2011. Degradation kinetics of azo dye reactive red SBE wastewater by complex ultraviolet and hydrogen peroxide process. Environ. Prog. Sustain. Energy 30, 208–215.

Xu, H.Z., Brookes, J., Hobson, P., Pei, H.Y., 2019. Impact of copper sulphate, potassium permanganate, and hydrogen peroxide on Pseudanabaena galeata cell integrity, release and degradation of 2-methylisoborneol. Water Res. 157, 64–73.

Yamashita, Y., Tanoue, E., 2003. Chemical characterization of protein-like fluorophores in DOM in relation to aromatic amino acids. Mar. Chem. 82, 255–271.

Yang, F., Sheng, B., Wang, Z.H., Xue, Y., Liu, J.S., Ma, T.Y., et al., 2021. Performance of UV/acetylacetone process for saline dye wastewater treatment: kinetics and mechanism. J. Hazard. Mater. 406, 124774.

Yang, M.H., Wu, B.D., Li, Q.H., Xiong, X.F., Zhang, H.R., Tian, Y., et al., 2018. Feasibility of the UV/AA process as a pretreatment approach for bioremediation of dye-laden wastewater. Chemosphere 194, 488–494.

Yilimulati, M., Jin, J.Y., Wang, X., Wang, X.M., Shevela, D., Wu, B., et al., 2021. Regulation of photosynthesis in bloom-forming cyanobacteria with the simplest β-diketone. Environ. Sci. Technol. 55, 14173–14184.

Yilimulati, M., Zhou, L., Shevela, D., Zhang, S.J., 2022. Acetylacetone interferes with carbon and nitrogen metabolism of microcystis aeruginosa by cutting off the electron flow to ferredoxin. Environ. Sci. Technol. 56 (13), 9683–9692.

Zhang, B.H., Ding, Z.G., Li, H.Q., Mou, X.Z., Zhang, Y.Q., Yang, J.Y., et al., 2016. Algicidal activity of streptomyces eurocidicus JXJ-0089 metabolites and their effects on microcystis physiology. Appl. Environ. Microbiol. 82, 5132–5143.

Zhang, C.C., Massey, I.Y., Liu, Y., Huang, F.Y., Gao, R.H., Ding, M., et al., 2019a. Identification and characterization of a novel indigenous algicidal bacterium Chryseobacterium species against *Microcystis aeruginosa*. J. Toxicol. Environ. Health, Part A 82, 845–853.

Zhang, D.W., Xie, P., Chen, J., 2010. Effects of temperature on the stability of microcystins in muscle of fish and its consequences for food safety. Bull. Environ. Contam. Toxicol. 84, 202–207.

Zhang, G.Y., Wu, B.D., Zhang, S.J., 2017. Effects of acetylacetone on the photoconversion of pharmaceuticals in natural and pure waters. Environ. Pollut. 225, 691–699.

Zhang, G.Y., Xie, M., Zhao, J., Wei, S.S., Zheng, H.C., Zhang, S.J., 2021. Key structural features that determine the selectivity of UV/acetylacetone for the degradation of aromatic pollutants when compared to UV/H_2O_2. Water Res. 196, 117046.

Zhang, H., Meng, G., Mao, F.J., Li, W.X., He, Y.L., Gin, K.Y.H., et al., 2019b. Use of an integrated metabolomics platform for mechanistic investigations of three commonly used algaecides on cyanobacterium, *Microcystis aeruginosa*. J. Hazard. Mater. 367, 120–127.

Zhang, L., Wu, B.D., Zhang, G.Y., Gan, Y.H., Zhang, S.J., 2019c. Enhanced decomplexation of Cu(II)-EDTA: the role of acetylacetone in Cu-mediated photo-Fenton reactions. Chem. Eng. J. 358, 1218–1226.

Zhang, S.J., Liu, X.T., Wang, M.S., Wu, B.D., Pan, B.C., Yang, H., et al., 2014. Diketone-mediated photochemical processes for target-selective degradation of dye pollutants. Environ. Sci. Technol. Lett. 1, 167–171.

Zhao, C.S., Shao, N.F., Yang, S.T., Ren, H., Ge, Y.R., Feng, P., et al., 2019. Predicting cyanobacteria bloom occurrence in lakes and reservoirs before blooms occur. Sci. Total Environ. 670, 837–848.

Zhou, S.Q., Shao, Y.S., Gao, N.Y., Deng, Y., Qiao, J.L., Ou, H.S., et al., 2013. Effects of different algaecides on the photosynthetic capacity, cell integrity and microcystin-LR release of *Microcystis aeruginosa*. Sci. Total Environ. 463, 111–119.